Significant differences among skeletal muscles in the incorporation of bone marrow-derived cells

Timothy R. Brazelton, Michael Nystrom, and Helen M. Blau*

Baxter Laboratory in Genetic Pharmacology, Stanford University School of Medicine, 269 W. Campus Drive, Stanford, CA 94305-5175, USA

Abstract

While numerous reports indicate that adult bone marrow-derived cells can contribute to nonhematopoietic tissues in vivo in adult mice, the generally low frequency of these events has made it difficult to study the molecular and cellular pathways involved. Here, we show a 1000-fold range in the frequency with which diverse skeletal muscles incorporate adult bone marrow-derived cells in adult mice. Most striking was the finding of one specific muscle, the panniculus carnosus, in which up to 5% of myofibers incorporated bone marrow-derived cells over a 16- month period in the absence of experimentally induced selective pressure. These results suggest that muscles differ physiologically, establishing the panniculus carnosus as an assay for identifying the key regulators, such as trophic, homing, and differentiation factors, as well as the relevant cells within the bone marrow that are capable of circulating throughout the periphery and contributing to adult, nonhematopoietic tissues, such as skeletal muscle. Finally, the 5% incorporation of adult stem cells into skeletal muscle is the highest reported to date in the absence of experimentally induced selective pressure and is at a level that may be consistent with improving the function of defective muscle tissue.
© 2003 Elsevier Inc. All rights reserved.

Introduction

Numerous discoveries in mice and humans during the last several years have demonstrated that circulating bone marrow-derived cells (BMDC) are able to contribute to various types of nonhematopoietic tissues in vivo, including neuronal cells in the CNS, skeletal muscle, endothelium, liver, and the epithelia of the gastrointestinal and respiratory tracts (Alison et al., 2000; Blau et al., 2001; Brazelton et al., 2000; Ferrari et al., 1998; Gussoni et al., 1999; Korbling et al., 2002; Krause et al., 2001; Okamoto et al., 2002; Orlic et al., 2001; Petersen et al., 1999; Priller et al., 2001; Theise et al., 2000; Weimann et al., 2003). However, due to the generally low frequencies of incorporation of BMDC into these tissues, it has been a subject of debate whether the proposed plasticity of adult bone marrow cells is physiologically relevant.

Here, we report a remarkably high 5% contribution of adult BMDC to an adult tissue in the absence of selective pressure induced genetically such as that resulting from heritable defects, or experimentally as a result of direct physical or toxic damage. For example, in the case of BMDC incorporation into liver, both types of selective pressure were involved (Lagasse et al., 2000; Petersen et al., 1999; Theise et al., 2000). Furthermore, we demonstrate that diverse skeletal muscles in mice range 1000-fold in the frequency with which they incorporate BMDC. The uptake of these cells can be substantial, and the differences among muscles are likely to have a physiological basis. As described previously (Brazelton et al., 2000), BMDC from a transgenic mouse ubiquitously expressing green fluorescent protein (GFP) are readily detectable in various adult tissues following bone marrow transplantation (BMT). Using this approach, we show here that in a subcutaneous muscle surrounding the trunk, the panniculus carnosus (PC, alternatively spelled "paniculus carnosus"), myofibers expressing GFP are detectable within weeks and comprise 1/20th of

* Corresponding author. Fax: +1-650-736-0080.
E-mail address: hblau@stanford.edu (H.M. Blau).

the total muscle fibers by 16 months after BMT. These data demonstrate that this is neither a rare nor subtle event, as large numbers of brightly fluorescent GFP+ fibers are observed per muscle.

The PC provides a convenient and useful assay for key trophic, homing, and differentiation factors responsible for BMDC incorporation in adult muscle. The range in frequencies, which span three orders of magnitude among the muscles reported here, suggests that BMDC may incorporate into muscles in a regulated manner according to need and that a comparison may shed light on the molecular basis for the observed differences in incorporation among muscles. Since the discordant observations regarding the differentiation potential of adult BMDC may well be due to the nature of the cell types tested (Blau et al., 2002; Brazelton et al., 2000; Castro et al., 2002; Wagers et al., 2002), the identification of the specific BMDC which contribute to myofibers in the PC will be of fundamental importance.

Materials and methods

Bone marrow transplantation (BMT)

Bone marrow was harvested from 8- to 10-week-old, male transgenic mice that ubiquitously expressed either enhanced green fluorescent protein (GFP) driven by a β-actin promoter and CMV enhancer (Okabe et al., 1997) or β-galactosidase (ROSA26 mice).

The marrow of 8- to 10-week-old, isogeneic C57B6 recipient mice was ablated by lethal irradiation (9.5 Gy), after which each mouse received 6×10^6 nucleated unfractionated bone marrow cells (expressing either GFP or β-galactosidase) by tail vein injection. By 8 weeks posttransplant, more than 95% of recipient mice exhibited GFP expression in $\geq$90% of their circulating, nucleated cells. Two of 43 groups of bone marrow-transplanted mice that had full reconstitution of their hematopoietic system with GFP-expressing cells failed to show incorporation of BMDC into the PC. Because this phenomenon occurred within all mice transplanted on the same day, it was likely the result of an essential but as of yet unidentified variable associated with the harvest and transplantation of the bone marrow at these times.

Muscle tissue preparation

At different time points posttransplant, recipient mice were sacrificed and intracardially perfused with sodium phosphate buffer followed by a freshly prepared solution of 1.5% paraformaldehyde and 0.1% glutaraldehyde. Tissues were then harvested, placed in 1.5% paraformaldehyde/ 0.1% glutaraldehyde/20% sucrose for 2 h, snap frozen, and cryosectioned to generate 20- to 50-μm-thick sections of fixed tissue.

Muscle survey

Three mice were sacrificed 16 months after receiving a BMT with unfractionated, GFP+ bone marrow and more than 70 skeletal muscles from each mouse were analyzed (listed in 26 groups in Table 1). The number of GFP+ myofibers was counted and the frequencies were compared for statistical significance by using the test for two proportions.

PC analysis

Sections of PC were harvested by drawing a grid on the shaved skin of an intact mouse (see Fig. 3a). First, five lines were drawn 0, 1, 2, 3, and 4 cm below the inferior angle of the scapulae and perpendicular to the spine. A vertical centerline was then drawn parallel to the spine. Four additional lines were drawn parallel to the spine 1 or 2 cm either to the left or right of the vertical centerline. The resulting 16 1×1-cm squares (4 rows of 4 squares) of skin were harvested individually.

For a comparison of the frequency of GFP+ myofibers among muscles, squares 3b and 3c were quantified (see Fig. 3a and Table 1)

For the time course, groups of three mice were harvested at various time points (2, 3, 5, 12, 16, 23, 50, and 78 weeks) and the PC muscle was evaluated for the presence of GFP+ myofibers. In all cases, the four squares in row 3 were evaluated (see Fig. 3a) with the sections cut perpendicular to the orientation of the myofibers. The resulting data were analyzed by standard linear regression.

Immunocytochemistry

Sections were stained with antibodies against muscle proteins, including myosin heavy chain (antibody A4.1025; recognizes all myosin heavy chain isoforms; Developmental Studies Hybridoma Bank, Iowa City, IA), desmin (Chemicon, Temecula, California), sarcomeric actin (Dako, Glostrup, Denmark), dystrophin (NovaCastra, Newcastle upon Tyne, United Kingdom), neural cell adhesion molecule (Pharmingen, San Diego, CA), and basal lamina components, such as laminin (Chemicon, Temecula, CA) and laminin-β2 (Upstate Biotechnology, Waltham, MA). Fiber types in the PC were evaluated by staining with antibodies to specific myosin heavy chain isoforms (all from DSHB, Iowa City, IA): A4.840 (Type 1, slow), A4.74 (Type IIa, fast), A4.1519 (Type II, fast), N3.36 (neonatal and Type II, neonatal and adult fast), and F1.652 (fetal) (Cho et al., 1993; Hughes and Blau, 1992; Hughes et al., 1993; Webster et al., 1988). In addition, Texas Red-conjugated α Bungarotoxin (Molecular Probes, Eugene, OR) was used to identify acetylcholine receptors. All sections were blocked with 20% normal goat serum, and those using anti- mouse secondary antibodies were blocked with saturating amounts of anti-CD16/32. Muscle sections stained with isotype control pri-

Table 1
Contribution of bone marrow cells to skeletal muscle

	Sixteen months post-BMT		
	Total fibers[b]	GFP+ fibers	Frequency
Muscle group			
Panniculus carnosus (4 cm)[a]	4,665[c]	152	3.26%
Panniculus carnosus (2 cm)[a]	5,852[c]	306	5.23%
Limbs			
Lower rear leg (total)	516,000	174	0.0337%
Biceps femoralis	29,000	3	0.0103%
Exten. digitorum longus	14,000	36	0.2571%
Exten. hallucis longus	23,000	10	0.0435%
Flexor digitorum longus	19,000	4	0.0211%
Flexor hallucis longus	13,000	5	0.0385%
Lateral gastrocnemius	67,000	28	0.0418%
Medial gastrocnemius	110,000	14	0.0127%
Peroneus brevis	28,000	15	0.0536%
Peroneus longus	20,000	4	0.0200%
Semimembranosus/semitendinosus	32,000	3	0.0094%
Soleus	37,000	4	0.0108%
Tibialis anterior	58,000	38	0.0655%
Tibialis posterior	66,000	10	0.0152%
Ankle/wrist[d]	130,000	13	0.0100%
Rear foot/toes[e]	4,100	0	—
Upper front leg[f]	27,000	97	0.3593%
Front foot[g]	39,000	1	0.0026%
Trunk			
Para-spinal[h]	910,000	161	0.0177%
Abdominal[i]	60,000	7	0.0117%
Ribs[j]	110,000	6	0.0055%
Irradiation controls			
Ear[k]	35,000	3	0.0086%
Tail[l]	4,500	0	—
Special			
Diaphragm[m]	930,000	26	0.0028%
Extra-ocular[m]	18,000	0	—
Tongue	180,000	4	0.0022%

Note. 1,000-fold differences in the frequencies of GFP-expressing myofibers in various muscles surveyed in three mice that were 16 months post-bone marrow transplant. "Irradiation controls" indicate skeletal muscle that received a full dose of irradiation that was unattenuated by overlying tissue and that did not have a significant increase in the number of GFP-expressing myofibers, suggesting that irradiation damage alone was not responsible for the differences in BMDC incorporation among muscles.

[a] Frequency of GFP-expressing myofibers was determined by sampling different widths of tissue samples as described in the methods and illustrated in Figure 3a.

[b] "Total fibers" calculated based on methods described in the appendix.

[c] Actual number of fibers counted.

[d] Ankle/wrist muscles include the distal extensions of most muscles of the lower front and back legs.

[e] The rear foot/toes include the flexor digiti quinti brevis, flexor hallucis brevis, adductor indicis, abductor digiti quinti, extensor digitorum brevis, flexor digitorum brevis, quadratus plantae, lumbricales, and the interossei plantares.

[f] Upper front leg muscles include the triceps brachi, dorsal latissimus dorsi, teres major, dorso-epitrochlearis brachil, biceps brachii, coracobrachialis, and the ventral tendon of the pectoralis.

[g] Front foot muscles include the abductor pollicis, flexor pollicis brevis, adductor pollicis, interossei, pisiform, abductor digiti quinti, flexor digiti quinti brevis, opponens digiti quinti, and the lumbricales

[h] Paraspinal muscles consisted primarily of erector spinae muscles (including illocostalis, longissimus, spinali) and psoas major & minor muscles but also included latissimus dorsi, levator claviculae, levator scapulae, longus capitis, longus colli, quadratus lumborumtrapezius, and rhomboideus.

[i] Abdominal muscles include the obliquus externus abdominis, obliquus internus abdominis, transversus abdominis, and the rectus abdomis.

[j] Rib sections were taken from the lateral thorax from the 7th-12th ribs. Muscles in this section include the intercostal muscles and serratus anterior.

[k] Ear muscles include the levator auris longus and the interscutularis plus unnamed myofiber bundles that acend into the ear from its base.

[l] Tail muscles consist of four bundles of myofibers which extend from the sacral and caudal vertebrae to the distal vertebrae of the tail. These are likely the extensor caudae externus and the extensor caudae internus described by Howell (1926).

[m] The extra-ocular muscles (EOM) are the group of six muscles that attach to the bulbar sheath and common annular tendon and which lie parallel to and surround the optic nerve.

mary antibodies and with appropriate secondary antibodies did not display positive staining. Unlike in LaBarge and Blau (2002), no antibodies were used to detect GFP. Although less sensitive than antibody staining, the direct detection of GFP emission reported here allows evaluation of a range of GFP levels not evident following antibody staining for GFP. This distinct methodology accounts for the difference in the frequency of BMDC incorporation into the tibialis anterior reported in Labarge and Blau, (2002).

Laser scanning confocal microscopic analysis

Each GFP+ cell was analyzed for GFP expression and/or antibody staining using epifluorescence and three-dimensional, confocal laser scanning microscopy (Zeiss LSM 510). The long pass filter set used for epifluorescent identification of GFP was a Chroma 41012 with HQ480/40 excitation, Q505LP split, and HQ510LP emission. Since this long pass filter set does not falsely change the hue of the observable emissions like a standard bandpass emission filter, GFP has a distinct hue compared with all sources of background autoflourescence. As a result, this filter set unequivocally distinguishes background from GFP. To capture the confocal images, each fluorophore was imaged individually to prevent cross detection of fluorophores. GFP was excited with 488-nm light from an Argon laser passed through a 488-nm bandpass filter and was detected after passing the emissions through a series of filters that included (in order) a 635-nm shortpass, 545 shortpass, and a 505–550 bandpass. Texas Red or Alexa 546 was excited with a 543-nm emission Helium–Neon (HeNe) laser passed through a 543-nm bandpass filter and was detected after passing the emissions through a 635-nm shortpass, 545 longpass, and a 560–615 bandpass. Cy5 was excited with a 633-nm HeNe laser passed though a 633-nm bandpass and was detected after the emissions were passed through a 635-nm longpass filter and a 650 long pass filter.

No GFP+ cells were seen in the muscles of control mice transplanted with unlabeled bone marrow cells. In order to demonstrate colocalization conclusively, confocal parameters were selected to minimize the thickness of the calculated optical section to 1–2 μm, despite the lower resolution images produced with these parameters.

Results

Bone marrow-derived cells contribute to skeletal myofibers in diverse muscles

Following lethal irradiation, recipient mice received intravenous injections of unfractionated bone marrow from an isogeneic, transgenic mouse that ubiquitously expresses enhanced GFP in most cell types, including all muscle cell types. When hematopoietic reconstitution was assessed 8 weeks posttransplant by flow cytometry, only mice with GFP expression in ≥90% of their circulating nucleated blood cells were analyzed further.

GFP+ fibers were identified as myofibers by their sarcomeric morphology, generally round borders by cross-sectional morphology, large volumes when analyzed in three dimensions, and high autofluorescence relative to other tissue and cell types, features that clearly distinguish them from blood vessels and individual blood cells (Fig. 1a–c). All myofibers were identified by three-dimensional analyses of a series of thin optical sections captured at different tissue depths using laser scanning confocal microscopy, which allowed visualization of the tube-like morphology of the myofibers even when analyzed in tissue sections cut perpendicular to the orientation of the myofibers (i.e., transverse sections). In an initial experiment, each GFP+ myofiber identified by these characteristics expressed one or more skeletal muscle-specific proteins in 200 myofibers in both the PC and the lower leg, providing strong validation for the identification criteria used in this report, as described below. Furthermore, in five mice transplanted with β-galactosidase-expressing bone marrow, no GFP-expressing myofibers or cells were observed in any muscle (data not

Fig. 1. Contribution of bone marrow-derived cells (BMDC) expressing GFP (green) to various skeletal muscles (red). (a–c) A cross-section of skin demonstrates the subdermal location of the panniculus carnosus (PC) muscle, which contains a relatively large proportion of GFP-expressing myofibers (>5%). The subdermal layer contains characteristically autofluorescent hair follicles (arrowheads, circular, red), small vessels (arrows), and a large number of small and irregular-shaped, GFP-expressing blood cells (green) are present in all layers, especially in the subdermal connective tissue and adipose layers. The individual fluorescence channels of the box in (a) are shown in (b) and (c). The myofiber identity of the eight GFP-expressing myofibers (asterisks, green) in (b) is demonstrated by the strong autofluorescent signals (c, red) characteristic of skeletal myofibers and hair follicles (arrowheads) but not blood vessels (arrows) in paraformaldehyde-fixed tissue. GFP-expressing fibers were identified as myofibers not only by autofluorescence but also by their generally round borders by cross-sectional morphology, and their sarcomeric morphology and large volumes which were visualized in three-dimensional image stacks captured with a laser scanning confocal microscope. Although the frequency differed 1000-fold, marrow-derived myofibers were observed in most muscles evaluated including in cross sections of the (d) triceps brachii and (e) extensor digitorum longus, and in longitudinal sections of the (f) tongue, (g) ear, and (h) serratus anterior muscles. (i, j) Low magnification images of whole mounts of the skin and diaphragm, respectively, demonstrate the abundance, characteristic length, and parallel orientation of GFP+ myofibers (green). Occasional branch points are present (arrowheads) are present in the PC (i). Darker areas are the result of mild hemorrhage or thicker adipose tissue that subtly attenuate the underlying GFP signal. Small GFP+ blood cells are evident particularly in the diaphragm, in which higher resolution images than in the PC were possible because of the abundance of refractile adipose tissue overlying the PC. No GFP myofibers nor cells were ever observed in tissue sections and whole mounts of skeletal muscles from mice successfully transplanted with LacZ-expressing bone marrow (data not shown). (BMDC are green and red autofluorescence highlights muscle tissue in all images). Scale bars in (a–h) indicate 50 μm and in (i, j) indicate 200 μm.
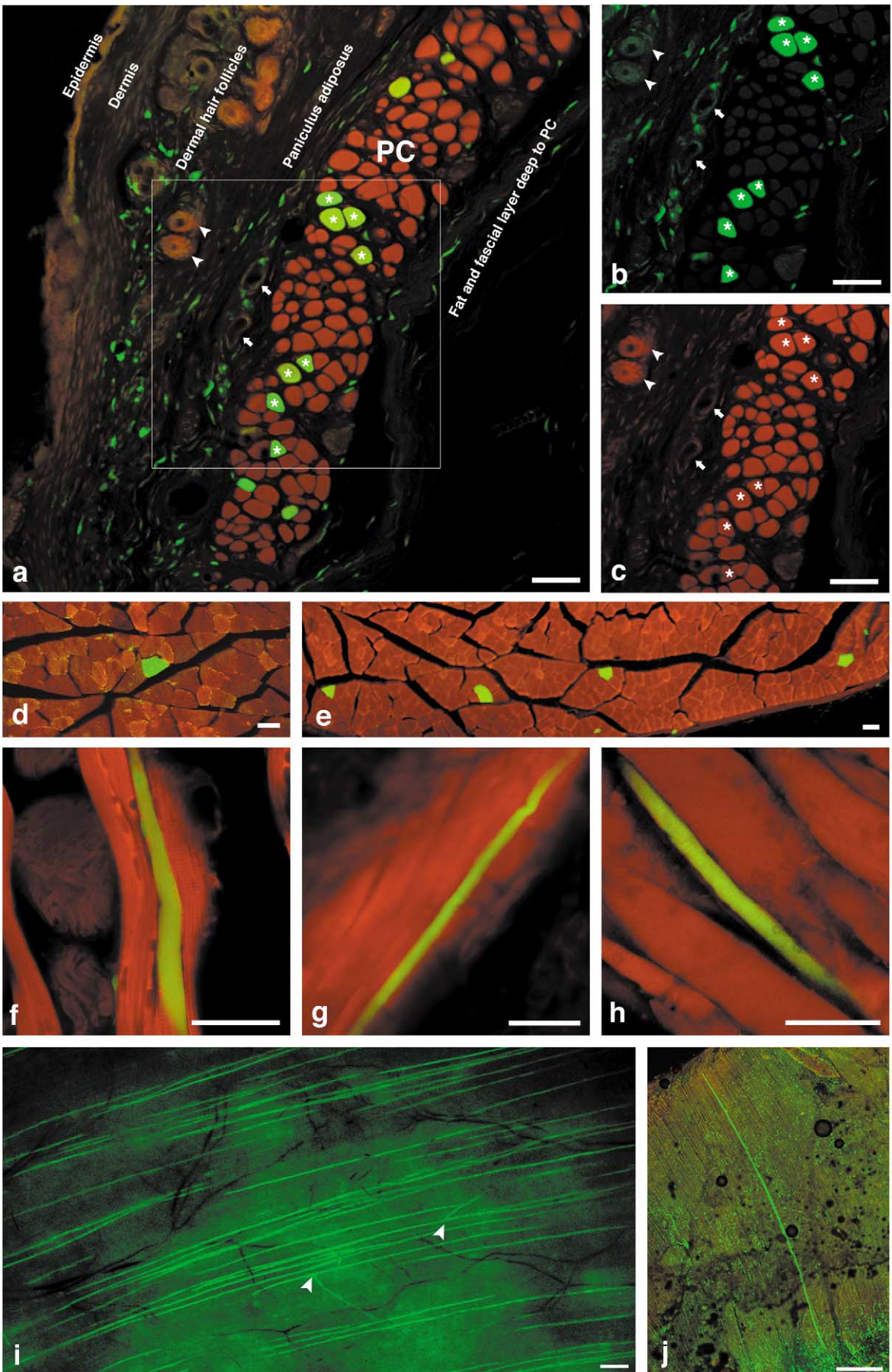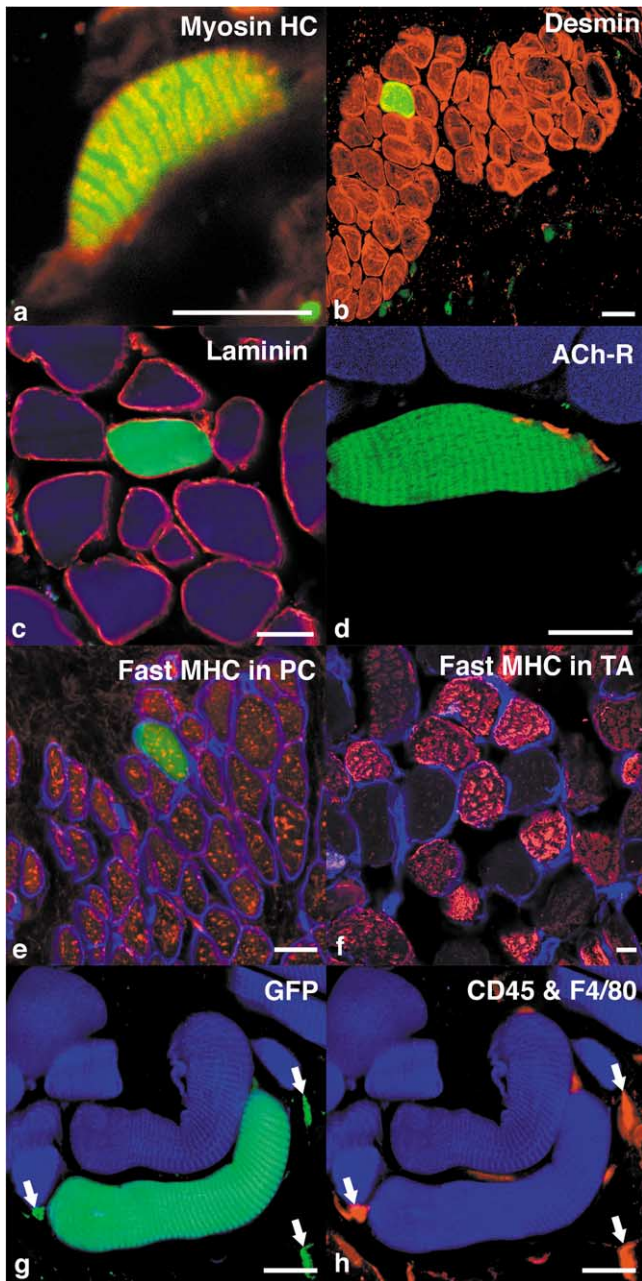
Fig. 2. Bone marrow-derived skeletal myofibers expressing GFP (green in all images) and costained with antibodies against characteristic proteins. All images are thin optical sections less than 5 μm thick that were captured by using laser scanning confocal microscopy to conclusively demonstrate colocalization. Blue in (c–d, g–h) is autofluorescence. Colocalization of red fluorophore and green GFP results in a yellow color. (a) Myosin heavy chain (red/yellow) and (b) desmin (red/yellow) indicate the expression of structural proteins typical of skeletal muscle. GFP-expressing myofibers have characteristic staining patterns on the cell surface for (c) laminin (red) and (d) acetylcholine receptor (red). At these sites of innervation, ACh-R are distributed in a cluster of circular patches on the membrane of the myofiber. In random, transverse sections of the PC, ACh-R patches were observed on 3.4% of non-GFP+ myofibers and 3.8% of GFP+ myofibers. (e, f) Myofibers identified by laminin beta-2 staining (blue) all express a fast specific isoform of myosin heavy chain (A4.1519, red) in the PC (e) whereas in the TA (f) only a subset of myofibers express fast myosin. (g, h) The expression of GFP and staining for both CD45 and F4/80 in a typical section of the PC is shown in (g) and (h), respectively (red in *h* is

shown), validating the specific detection of GFP by the imaging parameters.

Epifluorescent and laser scanning confocal analysis of 26 skeletal muscles or muscle groups distributed throughout the body resulted in the identification of skeletal myofibers expressing GFP in most muscles (Table 1). The morphology of the GFP+ myofibers was indistinguishable from that of their neighbors. GFP+ myofibers were always observed parallel to neighboring myofibers and were frequently greater than 10 mm in length.

At 4 and 16 months posttransplant, groups of three mice were euthanized, and skeletal muscles throughout each mouse were evaluated for the presence of GFP+ myofibers (Fig. 1a–h; Table 1, 4 month data not shown). Although the contribution of BMDC to skeletal myofibers was generally rare (<0.01–0.003%), the detection of GFP+ fibers provides evidence that a low level of repair is ongoing even in the absence of overt injury in most muscles. By 16 months posttransplant, several skeletal muscles in the lower leg had modest but reproducibly increased frequencies of BMDC-containing myofibers: the TA (0.07%), flexor hallucis longus (0.04%), and the lateral gastrocnemius (0.04%) (Table 1). However, by far the greatest frequency was observed in the panniculus carnosus (PC) in which 5.23% of myofibers expressed GFP. A second muscle with a relatively high frequency was the extensor digitorum longus (EDL; 0.26%). The incorporation of BMDC into these two muscles was highly significant compared to all other skeletal muscles analyzed ($P < 0.00001$ for both the EDL and PC; test for two proportions and Fisher exact test). In addition, the frequency of BMDC containing myofibers was significantly higher in the PC than in the extensor digitorum longus ($P = 0.0006$; test for two proportions). Thus, the PC incorporated BMDC into myofibers with a frequency 20-fold greater than that seen in the EDL, 340 times greater than that seen in the average skeletal muscle, and 1000-fold greater than the frequency seen in several other skeletal muscles (Table 1).

The PC muscle is a thin, subdermal, muscular layer within the superficial fascia that surrounds the entire trunk of animals with a hairy coat (Dorland, 1988) (Fig. 1a). As seen in Fig. 1a, the layers surrounding the PC, like most connective tissue layers in the bodies of these mice contain many small, elongated GFP+ blood cells that are clearly distinguishable from the skeletal myofibers. In the mice studied here, the PC has a width ranging from two to eight myofibers. Superficial to the PC is a well vascularized layer of fat and connective tissue, the panniculus adiposus, on top of which lies the dermis of the skin. Deep to the PC is another layer of fat and connective tissue under which is the

staining for pooled anti-CD45 and F4/80). No GFP+ skeletal myofibers but most GFP+ cells (i.e., blood cells) in skeletal muscle expressed either CD45 (h), a marker of hematopoietic cells, or F4/80 antigen (h), a marker of macrophages (arrows). Note clear sarcomeric distribution of GFP in (d) and (g). Scale bars indicate 20 μm.

potential space that separates when the skin is pulled away from the trunk. Thus, the superficial nature of the PC makes it readily accessible for experimental manipulation.

Certain muscle groups were hypothesized to show higher frequencies of BMDC incorporation into myofibers due to their higher contractile activity, but did not (Table 1). We reasoned that this might be the case for the extraocular muscles, which have drawn interest as they are spared in Duchenne muscular dystrophy and are characterized by an extraordinarily high rate of contraction, but no BMDC-containing myofibers were observed. Within the tongue, there was a marked tendency for GFP+ myofibers to occur within the centrally located rather than peripheral muscle fibers (0.01% for central myofibers vs. 0.005% GFP+ myofibers in the entire tongue) (Fig. 1f). In the diaphragm, which has a constant workload, the frequency (0.0028%) was actually reduced relative to other skeletal muscles despite the observation of several long GFP+ myofibers (Fig. 1f). These results suggest that characteristics other than contractile activity are inherent to certain muscles and are responsible for the differential frequency of BMDC incorporation.

GFP+ myofibers in the PC appear morphologically mature and express skeletal muscle-specific proteins

In order to better visualize the length of GFP+ myofibers in the PC, entire skins from five mice that were 10 months posttransplant were mounted intact between large glass plates and the interior surface of the pelt was evaluated. These GFP+ myofibers were frequently as long as other myofibers in their vicinity with an average length of 8 mm and with occasional fibers exceeding 30 mm (Fig. 1i). The arrowheads (Fig. 1i) indicate two myofiber branch points that were consistently found at low frequencies within such pelts.

The patterns of expression of several skeletal muscle-specific proteins together with the characteristic size and sarcomeric striations of myofibers confirmed that GFP+ myofibers were typical of differentiated skeletal muscle fibers. Sections of the PC and TA stained with antibodies to the muscle structural proteins myosin heavy chain (MHC) and desmin (Fig. 2a and b), as well as sarcomeric α-actin, and dystrophin (data not shown). In addition, each myofiber was ensheathed in laminin, a component of the muscle basal lamina (Fig. 2c). GFP+ myofibers also exhibited intact neuromuscular junctions when stained with Texas Red-labeled α-bungarotoxin, which binds to acetylcholine receptors (ACh-R) at neuromuscular junctions (Fig. 2d) (Sanes and Lichtman, 1999). Staining with five myosin-isoform specific antibodies (Cho et al., 1993; Hughes and Blau, 1992; Hughes et al., 1993; Webster et al., 1988) revealed that GFP+ myofibers, like all myofibers in the PC, homogeneously exhibited the same fast myosin fiber subtype. Specifically, PC myofibers labeled with two out of three antibodies to fast myosin isoforms tested (A4.1519+,

N3.36+, A4.74−) (Fig. 2e and f) but not with antibodies to slow (A4.840) nor fetal myosin (F1.652) (data not shown). In all cases, the patterns of antibody staining were indistinguishable from those seen in neighboring non-GFP+ myofibers. Importantly, GFP+ myofibers lacked expression of the blood lineage marker, CD45, which is expressed by almost all white blood cells, and the macrophage marker F4/80 (Fig. 2g and h), as well as the myeloid cell marker CD11b (data not shown). Thus, no proteins typical of bone marrow or circulating hematopoietic cells were observed in the GFP+ myofibers, all of which expressed characteristic muscle proteins and exhibited striations typical of contractile sarcomeres.

GFP+ myofibers are formed continuously over time

Although the PC surrounds the entire trunk of the mouse, two specific areas within the PC contain the vast majority of GFP+ myofibers in this muscle (Fig. 3a). A time course (Fig. 3b), in which regions A-D of row 3 were scored (Fig. 3a), revealed that GFP+ myofiber formation was not an acute response but increased continuously in an approximately linear manner ($R^2 = 0.73$). GFP+ myofibers were seen as early as 3 weeks post-BMT, although they were extremely rare at this time point. By 16 weeks post-BMT, the average lumbar strip of PC (row 3 in Fig. 3a) contained 10 GFP+ myofibers, or 0.5 ± 0.3% of the total, suggesting that the sensitivity of this assay would suffice at this time point. Furthermore, the linear increase is suggestive of a physiological process in which BMDC continually contribute to myofibers, providing a source of cells to meet the need for myofiber replenishment over time.

The PC is a highly regenerative skeletal muscle

The main distinction between the PC and the other muscles examined is its regenerative activity. Two morphological features are characteristic of myofiber regeneration in postnatal skeletal muscle: heterogeneous fiber diameters and centrally located nuclei (Grounds et al., 1980) (Fig. 4a, arrows and arrowheads). The incidence of central nucleation is significantly increased in the PC myofibers of both BMT mice and age-matched, nontransplanted mice ($P < 0.0001$ for either compared with TA; Fig. 4a and b). Within the PC of BMT mice, 31% of nuclei in GFP+ myofibers are centrally located.

This frequency is 2.5-fold the frequency observed both in GFP-negative myofibers in the PC of the same mice (13%) and in control, PC myofibers in nonirradiated, non- BMT age-matched mice (12%). It is noteworthy that, in most skeletal muscles, like the TA, no fibers with centrally located nuclei are observed in the absence of damage such as needle stab injury (Grounds et al., 1980; Heslop et al., 2000). In addition, in both nontransplanted and BMT mice, the PC exhibits increased myofiber heterogeneity and a smaller mean fiber diameter compared with normal TA (*P*

< 0.0001 for both groups) (Fig. 4c). Moreover, the population of GFP+ fiber diameters exhibits an increased heterogeneity and a significant shift toward smaller fiber sizes ($P < 0.001$) relative to non- GFP-expressing myofibers in the PC (Fig. 4c.5 and c.6) and is similar to that seen in the regenerating TA (Fig. 4c.2). Both the heterogeneous myofiber morphology and increased frequency of centrally located nuclei suggest that the PC is a skeletal muscle with increased regeneration compared to other skeletal muscles.

Discussion

We show here that, in contrast to most previous reports, the contribution of BMDC to nonhematopoietic tissues can be both readily apparent and, in some cases, strikingly robust. Indeed, incorporation of BMDC into one tissue, skeletal muscle, can differ 1000-fold. In some muscles, as little as 0.002% (tongue, intercostal muscles) of the muscle fibers contained nuclei from GFP+ BMDC, whereas in others, such as the EDL and PC, the frequency was as high as 0.26 and 5.2%, respectively. The large range in the frequencies of BMDC contribution to GFP+ fibers suggests that there is a biological basis for this difference.

The differences in BMDC incorporation observed among muscles may well relate to the high regenerative activity of the PC relative to most skeletal muscles. Indeed, the PC has several characteristics of regenerated skeletal muscle, including significantly smaller fiber diameters, increased heterogeneity of fiber sizes, and an unusually high percentage of centrally nucleated myofibers in the absence of focal injury. By contrast, in muscles such as the tibialis anterior (TA) and diaphragm, which are not highly regenerative in these mice, no centrally located nuclei were observed and only 0.07 and 0.003% of myofibers expressed GFP, respectively, unless damage is induced, leading to regeneration and repair (Fig. 4c.2). It is well known that increased exercise, an inducer of damage and regeneration, increases myofiber heterogeneity and centrally located nuclei in skeletal muscles (Grounds, 1998). Moreover, muscles which normally exhibit a low frequency of BMDC incorporation relative to the PC, can be induced to take up these cells at higher frequencies following an intense 6-month, exercise-induced, damage regimen (LaBarge and Blau, 2002). Thus, an increased rate of myofiber regeneration in the PC, relative to other muscles, may explain, at least in part, the exceptionally high rate of BMDC incorporation into the PC.

Although the PC has not been extensively studied, additional observations distinguish it from typical skeletal muscles. The PC is reported to be a site of exceptionally rapid wound healing and angiogenesis (Munz et al., 1999) and has a plentiful blood supply from overlying dermal vessels. Furthermore, it has been hypothesized that the PC plays a role in maintaining temperature homeostasis (Dark, 2002), which implies a potentially high contractile activity and is consistent with the fast myofiber types observed. Thus, in addition to its high regenerative activity, the PC may be unique in other properties relevant to the incorporation of BMDC.

Several observations suggest that the results reported in the PC are not a consequence of the marrow-ablating irradiation protocol which is necessary for bone marrow transplantation and which could, in theory, have contributed to the high level of BMDC incorporation into the PC. First, radiation might have increased regeneration in the PC. This does not appear to be the case since myofiber size and nuclear location in the PC are similar in age-matched, non-irradiated controls and in irradiated BMT mice ($P = 0.27$). Second, irradiation exposure may have differed in the PC relative to other muscles. However, tissues at all depths of the mice received essentially the same radiation dose because the gamma radiation used is minimally attenuated by tissue: less than 1 and 5% attenuation per inch for soft tissue and solid bone, respectively (Wright, 1992). Furthermore, the maximum beam angle used ($15°$ from vertical) results in a negligible decrease in irradiation due to beam spreading. In addition, muscles on the dorsal surface of the mice, including the PC on the cranium and neck as well as the muscles of the ear and tail (Table 1, irradiation controls), did not show enhanced regeneration and serve as internal controls for irradiation intensity. Thus, irradiation is unlikely to account for the observed effects, as the PC did not receive significantly higher levels of irradiation than deeper skeletal muscles.

Irrespective of the physiological basis for the observed differences, the PC provides an assay system for detecting regulatory factors that are responsible for the increased uptake of BMDC. For example, well-characterized factors could be administered to the PC to determine whether they alter the frequency of incorporation or, if administered to other skeletal muscles, if they allow non-PC muscles to reach a level of myofiber regeneration comparable to the PC. In addition, screens for novel factors could be developed based on the striking differences in incorporation of BMDC into the PC compared with the TA using comparative approaches such as microarrays or subtractive cDNA libraries. At this time, the pathways regulating the incorporation of BMDC into skeletal muscles are unknown and, although some known molecular players will likely be involved, the elucidation of these regulatory mechanisms will be essential to the development of therapeutic strategies for regenerative medicine.

The PC has several advantages as an assay system. The superficial position of the PC makes it accessible for experimental manipulations such as the direct administration of experimental factors or through the use of standard murine injury models. Furthermore, its accessibility combined with its nonessential function allows multiple biopsies to be taken from a single mouse over time. The frequencies of GFP+ myofibers are well suited to the sensitive and statistically significant detection of factors that either increase or decrease the incorporation of BMDC. Importantly, since the
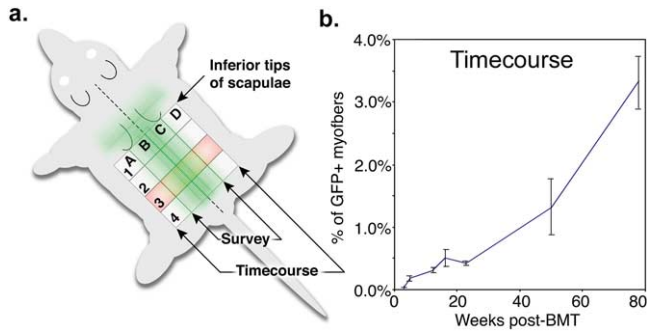
Fig. 3. (a) Illustration of the two specific areas within the PC with the highest densities of GFP+ myofibers. The first is an approximately 2-cm-wide strip centered over and parallel to the lumbar spine and extending from the inferior angle of the scapula to the mid-pelvis. The second area encompassed an approximately 2-cm-wide strip, perpendicular to the spine, with the midline of the strip centered over the scapular spines. In this area, the myofibers run at a right angle to the spine and the area of increased GFP+ myofibers extends approximately 3 cm to either side of the spine (in skin mounted between glass). The margins of these areas, while approximate, were consistent in the 24 mice evaluated using whole skin mounts. In areas of the PC outside of these regions, occasional GFP+ myofibers were observed but at a substantially reduced frequency. Samples of the PC were collected by drawing a 4 × 4-cm square grid centered on the spine (dotted line) with the top row just below the inferior angles of the scapulae. Note that squares 3A and 3B were analyzed for the muscle survey whereas for the time course analysis all four squares in row 3 were analyzed. (b) Time-dependent increase in GFP+ skeletal myofibers in the panniculus carnosus continues for over a year after bone marrow transplantation. Each time point represents a group of 3 mice. The reproducibility and consistency of the assay are demonstrated by the relatively small standard deviations for each time point, an essential characteristic for an assay system.

high frequency of BMDC incorporation into the PC occurs in the absence of selective pressure that is induced experimentally or by genetic damage, the effects of experimental manipulations will be easier to interpret and more likely to be of biological and physiological relevance.

In summary, skeletal muscles differ over 1000-fold in the frequency of BMDC incorporation, suggesting that the ability of adult stem cells to contribute to non- hematopoietic tissue is a regulated process and that modifiers of this process may allow greatly enhanced tissue regeneration from adult stem cells. Indeed, the incorporation of BMDC into more than 5% of myofibers is the highest frequency reported to date for skeletal muscle and suggests that BMDC may be able to incorporate at a level capable of changing the physiology of tissues such as muscle. Our data suggest that a marrow associated regenerative cell may well be capable of serving as a back-up or regenerative reservoir when there is a physiologic or injury-induced need that cannot be met by local stem cells residing within tissues. How or whether such cells are related to other cells defined within bone marrow, such as the hematopoietic stem cells or marrow stromal cells, remains to be determined. A better understanding and characterization of the factors that may be involved in recruiting and converting BMDC to nonhematopoietic fates may ultimately lead to novel therapeutic
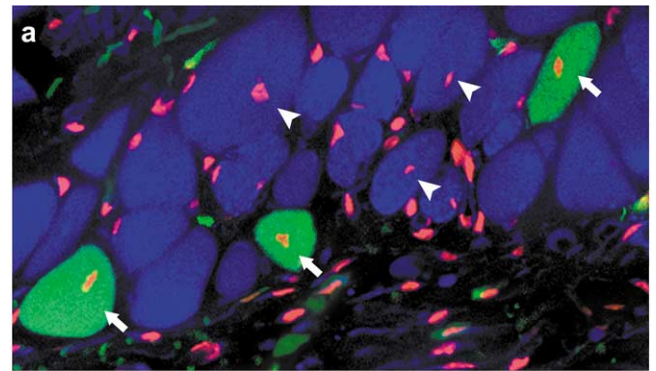
b. Location of nuclei in myofibers

Group	Peripheral	Central	Percent central	
Native TA myofibers	54	0	0%	
Native PC myofibers	238	32	12%	} P=0.27
BMT PC (all fibers)	247	45	15%	
GFP+ fibers in BMT PC	58	26	**31%**	} P=0.0004
GFP(-) fibers in BMT PC	226	34	**13%**	

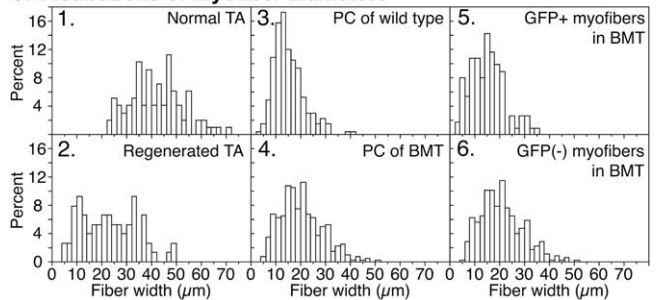**c. Distributions of myofiber diameters**

Fig. 4. (a, b) The frequency of centrally located nuclei (red) was increased within GFP+ myofibers, an indicator of myofiber regeneration. In these images, which were captured with a confocal microscope, the optical thickness of each image is 2-3 μm. All myofibers were assessed for nuclear location by using a three-dimensional analysis of a stack of thin optical sections and nuclei were required to be contained within the three- dimensional volume of the myofiber in order to be counted. Thus, nuclei in (a) which appear centrally located in GFP+ (arrows) and non-GFP expressing (arrowheads) myofibers are unquestionably myonuclei contained within the myofibers and not overlying blood cell nuclei. Several mononuclear cell nuclei, including some in GFP- expressing mononuclear cells, are present above and below the PC muscle layer. (b) Increased incidence of central nucleation following skeletal muscle regeneration in three groups of three mice each. Nuclei in myofibers of the tibialis anterior (TA) of normal mice are located primarily in the periphery, whereas an increase in the proportion of centrally located nuclei, characteristic of regenerated skeletal muscle, is observed in the panniculus carnosus (PC) of both normal and bone marrow-transplanted mice. Central nucleation is also significantly increased in GFP+ myofibers compared with non-GFP- expressing myofibers in mice that received a bone marrow transplant from a GFP-expressing donor. (c) Comparative distributions of myofiber sizes demonstrate the heterogeneity in the PC relative to the TA in four groups of three mice each. (c.1 and c.2) The decrease in mean myofiber size and the increase in fiber size heterogeneity in the PC is similar to regenerated (needle track injured) tibialis anterior (TA). (c.3 and c.4) PC myofibers in age-matched wild type and irradiated bone marrow-transplanted (BMT) mice are remarkably similar. (c.5 and c.6) The population of GFP-expressing myofibers in the PC exhibits a significant shift toward smaller fiber sizes (P < 0.001) relative to non- GFP-expressing myoblasts. These data demonstrate the intrinsic regenerative nature of the PC relative to the TA muscle.

strategies in which the endogenous BMDC of an individual are enlisted to contribute to specific regenerative process as needed.

Appendix

Bone marrow transplantation (BMT)

BM was harvested from 8- to 10-week-old, male transgenic mice that ubiquitously expressed an enhanced version of green fluorescent protein (GFP) driven with a B-actin promoter and a CMV enhancer. Briefly, donor mice were euthanized by cervical dislocation, immersed in 70% ethanol, and the skin was peeled back from a midline, circumferential incision. Large limb bones (femur, tibia, and humerus) were surgically isolated and placed in ice-cold calcium and magnesium-free, Hank's balanced salt solution (HBSS, Irvine Scientific) with 2% FBS for up to 90 min. In a tissue culture hood, the tips of the bones were removed and a 25-gauge needle containing 1 mL of ice-cold HBSS with 2% FCS was inserted into the marrow cavity and used to wash the marrow out into a sterile culture dish. Marrow fragments were dissociated by titurating through the 25-gauge needle and the resulting suspension was filtered through sterile 70-μm nitex mesh. The filtrate was cooled on ice, spun for 5 min at $250g$, and the pellet was resuspended in ice-cold HBSS with 2% FCS to 4.8×10^7 nucleated cells per mL.

The marrow of 8- to 10-week-old, isogeneic (C57B/6, Stanford), recipient mice was ablated by lethal irradiation (two doses of 475 cGy, 3 h apart). Within the 3 h following lethal irradiation, each mouse received 6×10^6 nucleated whole BM cells (in 125 μL HBSS) by tail vein injection. Following the transplant, mice were maintained under standard conditions with a constantly maintained temperature of 20–22°C.

Hematopoietic reconstitution was assayed 8 weeks post-transplant by flow cytometric evaluation of the frequency of GFP+ circulating cells. By 8 weeks post-transplant, over 95% of recipient mice expressed GFP in greater than 90% of their circulating, nucleated cells. Only mice meeting this criterion were analyzed further.

Tissue collection

At varying times post-transplant, recipient mice were anesthetized with 60 mg/kg Nembutol and intracardially perfused with 30 mL of 0°C sodium phosphate buffer (PB, pH 7.4) followed by 30 mL of 0°C 1.5% freshly dissolved paraformaldehyde (PF) and 0.1% glutaraldehyde. Tissues were harvested, placed in 1.5% PF/0.1% glutaraldehyde/ 20% sucrose at 4°C for 2 h and snap frozen in TISSUE-TEK O.C.T. compound (Sakura Finetek). 20- to 50-μm-thick sections of fixed tissue from over 70 skeletal muscles were cut perpendicular to the orientation of the myofibers on a cryostat.

Muscle survey

Individual muscles were identified and the number and location of each GFP+ myofiber, as well as the total number of myofibers in that muscle, were recorded. Although all GFP+ fibers were counted, in most muscles other than the PC the total number of myofibers present was calculated by counting approximately 1000 fibers, measuring the total area of those fibers, and then extrapolating that number for the total area of that muscle with identical myofiber orientation. All muscles were analyzed in three mice, each harvested at 4 and 16 months post-BMT. The frequencies of GFP+ myofibers were compared for statistical significance using the test for two proportions.

References

Alison, M.R., Poulsom, R., Jeffery, R., Dhillon, A.P., Quaglia, A., Jacob, J., Novelli, M., Prentice, G., Williamson, J., Wright, N.A., 2000. Hepatocytes from non-hepatic adult stem cells. Nature 406, 257.

Blau, H., Brazelton, T., Keshet, G., Rossi, F., 2002. Something in the eye of the beholder. Science 298, 301–362 discussion 302–363.

Blau, H.M., Brazelton, T.R., Weimann, J.M., 2001. The evolving concept of a stem cell: entity or function? Cell 105, 829–841.

Brazelton, T.R., Rossi, F.M., Keshet, G.I., Blau, H.M., 2000. From marrow to brain: expression of neuronal phenotypes in adult mice. Science 290, 1775–1779.

Castro, R.F., Jackson, K.A., Goodell, M.A., Robertson, C.S., Liu, H., Shine, H.D., 2002. Failure of bone marrow cells to transdifferentiate into neural cells in vivo. Science 297, 1299.

Cho, M., Webster, S.G., Blau, H.M., 1993. Evidence for myoblast-extrinsic regulation of slow myosin heavy chain expression during muscle fiber formation in embryonic development. J. Cell Biol. 121, 795–810.

Dark, G., 2002. The On-Line Medical Dictionary. CancerWEB, UK & Academic Medical Publishing.

Dorland. 1988. Dorland's Illustrated Medical Dictionary. W.B. Saunders Company, Philadelphia.

Ferrari, G., Cusella-De Angelis, G., Coletta, M., Paolucci, E., Stornaiuolo, A., Cossu, G., Mavilio, F., 1998. Muscle regeneration by bone marrow-derived myogenic progenitors. Science 279, 1528–1530.

Grounds, M., Partridge, T.A., Sloper, J.C., 1980. The contribution of exogenous cells to regenerating skeletal muscle: an isoenzyme study of muscle allografts in mice. J. Pathol. 132, 325–341.

Grounds, M.D., 1998. Age-associated changes in the response of skeletal muscle cells to exercise and regeneration. Ann. N. Y. Acad. Sci. 854, 78–91.

Gussoni, E., Soneoka, Y., Strickland, C.D., Buzney, E.A., Khan, M.K., Flint, A.F., Kunkel, L.M., Mulligan, R.C., 1999. Dystrophin expression in the mdx mouse restored by stem cell transplantation. Nature 401, 390–394.

Heslop, L., Morgan, J.E., Partridge, T.A., 2000. Evidence for a myogenic stem cell that is exhausted in dystrophic muscle. J. Cell Sci. 113, 2299–2308.

Hughes, S.M., Blau, H.M., 1992. Muscle fiber pattern is independent of cell lineage in postnatal rodent development. Cell 68, 659–671.

Hughes, S.M., Cho, M., Karsch-Mizrachi, I., Travis, M., Silberstein, L., Leinwand, L.A., Blau, H.M., 1993. Three slow myosin heavy chains sequentially expressed in developing mammalian skeletal muscle. Dev. Biol. 158, 183–199.

Korbling, M., Katz, R.L., Khanna, A., Ruifrok, A.C., Rondon, G., Albitar, M., Champlin, R.E., Estrov, Z., 2002. Hepatocytes and epithelial cells of donor origin in recipients of peripheral-blood stem cells. N. Engl. J. Med. 346, 738–746.

Krause, D.S., Theise, N.D., Collector, M.I., Henegariu, O., Hwang, S., Gardner, R., Neutzel, S., Sharkis, S.J., 2001. Multi-organ, multi-lineage engraftment by a single bone marrow-derived stem cell. Cell 105, 369–377.

LaBarge, M.A., Blau, H.M., 2002. Biological progression from adult bone marrow to mononucleate muscle stem cell to multinucleate muscle fiber in response to injury. Cell 111, 589–601.

Lagasse, E., Connors, H., Al-Dhalimy, M., Reitsma, M., Dohse, M., Osborne, L., Wang, X., Finegold, M., Weissman, I.L., Grompe, M., 2000. Purified hematopoietic stem cells can differentiate into hepatocytes in vivo. Nat. Med. 6, 1229–1234.

Munz, B., Wiedmann, M., Lochmuller, H., Werner, S., 1999. Cloning of novel injury-regulated genes. Implications for an important role of the muscle-specific protein skNAC in muscle repair. J. Biol. Chem. 274, 13305–13310.

Okabe, M., Ikawa, M., Kominami, K., Nakanishi, T., Nishimune, Y., 1997. "Green mice" as a source of ubiquitous green cells. FEBS Lett. 407, 313–319.

Okamoto, R., Yajima, T., Yamazaki, M., Kanai, T., Mukai, M., Okamoto, S., Ikeda, Y., Hibi, T., Inazawa, J., Watanabe, M., 2002. Damaged epithelia regenerated by bone marrow-derived cells in the human gastrointestinal tract. Nat. Med. 8, 1011–1017.

Orlic, D., Kajstura, J., Chimenti, S., Jakoniuk, I., Anderson, S.M., Li, B., Pickel, J., McKay, R., Nadal-Ginard, B., Bodine, D.M., Leri, A., Anversa, P., 2001. Bone marrow cells regenerate infarcted myocardium. Nature 410, 701–705.

Petersen, B.E., Bowen, W.C., Patrene, K.D., Mars, W.M., Sullivan, A.K., Murase, N., Boggs, S.S., Greenberger, J.S., Goff, J.P., 1999. Bone marrow as a potential source of hepatic oval cells. Science 284, 1168–1170.

Priller, J., Persons, D.A., Klett, F.F., Kempermann, G., Kreutzberg, G.W., Dirnagl, U., 2001. Neogenesis of cerebellar Purkinje neurons from gene-marked bone marrow cells in vivo. J. Cell Biol. 155, 733–738.

Sanes, J.R., Lichtman, J.W., 1999. Development of the vertebrate neuromuscular junction. Annu. Rev. Neurosci. 22, 389–442.

Theise, N.D., Badve, S., Saxena, R., Henegariu, O., Sell, S., Crawford, J.M., Krause, D.S., 2000. Derivation of hepatocytes from bone marrow cells in mice after radiation-induced myeloablation. Hepatology 31, 235–240.

Wagers, A.J., Sherwood, R.I., Christensen, J.L., Weissman, I.L., 2002. Little evidence for developmental plasticity of adult hematopoietic stem cells. Science 297, 2256–2259.

Webster, C., Silberstein, L., Hays, A.P., Blau, H.M., 1988. Fast muscle fibers are preferentially affected in Duchenne muscular dystrophy. Cell 52, 503–513.

Weimann, J.M., Charlton, C.A., Brazelton, T.R., Hackman, R.C., Blau, H.M. 2003. Contribution of transplanted bone marrow cells to Purkinje neurons in human adult brains. Proc. Natl. Acad. Sci. USA, in press.

Wright, A.E., 1992. Medical Physics Handbook of Radiation Therapy. Medical Physics Publ, Madison, WI.